THE UNIVERSITY OF CHICAGO PRESS JOURNALS

Accuracy and Covariance Analysis of Global Astrometry with the *Space Interferometry Mission*

Author(s): Valeri V. Makarov and Mark Milman

Source: *Publications of the Astronomical Society of the Pacific*, Vol. 117, No. 833 (July 2005), pp. 757-771
Published by: Astronomical Society of the Pacific
Stable URL: http://www.jstor.org/stable/10.1086/431367
Accessed: 18-11-2016 23:40 UTC

JSTOR is a not-for-profit service that helps scholars, researchers, and students discover, use, and build upon a wide range of content in a trusted digital archive. We use information technology and tools to increase productivity and facilitate new forms of scholarship. For more information about JSTOR, please contact support@jstor.org.

Your use of the JSTOR archive indicates your acceptance of the Terms & Conditions of Use, available at http://about.jstor.org/terms

Astronomical Society of the Pacific, The University of Chicago Press are collaborating with JSTOR to digitize, preserve and extend access to *Publications of the Astronomical Society of the Pacific*

This content downloaded from 150.135.211.221 on Fri, 18 Nov 2016 23:40:02 UTC
All use subject to http://about.jstor.org/terms

Publications of the Astronomical Society of the Pacific, **117**:757–771, 2005 July
© 2005. The Astronomical Society of the Pacific. All rights reserved. Printed in U.S.A.

Accuracy and Covariance Analysis of Global Astrometry with the *Space Interferometry Mission*

Valeri V. Makarov[1,2] and Mark Milman[2]
Received 2005 March 18; accepted 2005 April 27; published 2005 June 23

ABSTRACT. Construction of an all-sky microarcsecond astrometric grid is an essential preliminary step toward global astrometry with the *Space Interferometry Mission* (*SIM*). The general setup of the global astrometry problem is given, and fast, robust algorithms to solve the problem are described. The results of extensive numerical simulations are used to outline the conditions necessary to achieve the performance goal of absolute astrometric accuracy. Rigorous computation of the global covariance matrix makes it possible to correctly interpret and utilize the *SIM* data. We formulate and resolve the new issue of the basic performance uncertainty of a single astrometric mission.

1. INTRODUCTION

The *Space Interferometry Mission* (*SIM*) is a cornerstone project in the NASA Origins Program. It is mainly dedicated to the search for extrasolar planetary systems, but its astrophysical agenda also comprises a range of key projects related to Galactic dynamics, star formation, astrometric reference systems, etc. (Unwin & Shao 2000). One of the main objectives of the mission is to achieve a 4 μas accuracy of parallaxes of target stars during a 5 year operation. This will ensure a similar, or better, accuracy of mean positions and proper motions, provided the stars are nonbinary and nonaccelerating.

The *SIM* instrument is a system of four mutually connected Michelson-type interferometers with roughly parallel baselines (Shao 1998). One of these interferometers with the longer 10 m baseline is dedicated to observations of science stars, and two others with shorter baselines of about 8 m will only observe bright guide stars for calibration purposes. The fourth interferometer is a redundant science interferometer. The purpose of the guide interferometers is to monitor (regularize) the path delay of the science interferometer in use in such a way that its baseline orientation can be considered as "fixed" in inertial space to sufficient accuracy during the set of science observations made over the 15° field of regard (FOR) of the instrument. The observations made within a single field of regard (also termed a "tile") include delay measurements of grid stars that are used to define the global reference system, as well as the target stars that have been selected for *SIM*'s various science investigations. The whole mission is a series of intermittent tile observations separated by shorter reorientation maneuvers and technical cycles. The science interferometer typically observes all targets and grid stars of the tile in about 1 hr. Although the baseline is virtually static, owing to the path delay regularization with the guide interferometers, the baseline orientation with respect to stars is not known a priori to sufficient accuracy.

Along with other instrument parameters, the baseline orientation (attitude) is derived from grid star measurements with the science interferometer. Hence, the instrument calibration is a two-stage process: (1) regularization of the science path delays using the guide interferometers and the metrology subsystems on the timescale of one tile, and (2) determination of baseline attitude and instrument parameters in on-ground data reductions. The former technique is described in Milman & Turyshev (2000). The latter is an inherent part of the global astrometric solution of grid stars, which is the subject of this paper. The description of the extensive development and verification of technologies required by *SIM* can be found in Laskin (2003).

SIM has an important methodological difference from the successful *Hipparcos* mission (ESA 1997). *SIM* observes in just one direction at a time, while *Hipparcos* was equipped with a calibrated basic angle allowing quasi-simultaneous measurements of stars separated by ≈58°. In the *SIM* global solution, a large number of overlapping tiles have to be tied up to construct an accurate astrometric grid covering the entire sky. The technique is somewhat similar to the all-sky astrometric reduction of overlapping plates (Eichhorn 1960; Jefferys 1963; Googe et al. 1970; de Vegt & Ebner 1974), in which large systems of equations have to be solved by the elimination of plate parameters in each block (N. Zacharias 2003, private communication). The lack of a wide basic angle causes some additional loss of condition, partly compensated by a rather wide FOR of 15° diameter. The *Hipparcos* mean parallaxes of a few open clusters are known to be in error, most notably for the Pleiades (Pinsonneault et al. 1998). The crux of the matter is that the mean parallax of some 50 member stars with individual parallax errors of 1–2 mas differs from the true value by about 1 mas, which is ≈5 formal standard errors, under the assumption

[1] Michelson Science Center, California Institute of Technology, 770 South Wilson Avenue, Mail Stop 100-22, Pasadena, CA 91125; valeri.makarov@jpl.nasa.gov.

[2] Jet Propulsion Laboratory, 4800 Oak Grove Drive, Pasadena, CA 91109-8099.

This content downloaded from 150.135.211.221 on Fri, 18 Nov 2016 23:40:02 UTC
All use subject to http://about.jstor.org/terms

that the individual parallaxes are uncorrelated. This implies that the parallax errors in *Hipparcos* are in fact positively correlated, and perhaps strongly so. It has been shown that the likely cause of the correlated errors was the propagation of random errors in the overparameterized attitude model that was allowed to accommodate high-frequency wiggles (Makarov 2002). Restating the observational equations so that the attitude unknowns are effectively eliminated brings about a remarkable reduction of the correlated error; consequently, a reproduction of the entire *Hipparcos* catalog has been suggested (Makarov 2003).

From a practical point of view, no controversy would ever emerge if the standard deviation of the mean parallax could be correctly calculated from the full covariance matrix of astrometric parameters including star-to-star covariances. A preliminary covariance study would have revealed the large positive correlations between astrometric parameters, and at the very least, the computed formal error of the mean parallax would have been consistent with the actual offset. In fact, there are strong indications that the problem could be fixed by choosing a different algorithm of astrometric data reduction. The full covariance matrix could not be computed in *Hipparcos*, since the adopted solution was not global, but rather a three-step iterative procedure including the adjustment of one-dimensional abscissae coordinates and attitude (great circle reductions), adjustment of reference great circle zero points, and finally, a fit to astrometric parameters over the entire set of the great circle abscissae (sphere solution). The main reason for using this scheme was the practical difficulty of a least-squares solution on a global design matrix of over 6×10^5 unknowns (Lattanzi et al. 1990).

The global solution was investigated by numerical simulations in the framework of the *Hipparcos* mission and was found to yield a significantly more precise result (Bucciarelli et al. 1991). It appears quite likely, although it has not been proven, that the gain in precision is due to improved spatial correlations between close stars. One might speculate that the gain was due to a more rigorous treatment of the attitude parameters, thus avoiding the spatially correlated errors on an intermediate scale. For the *SIM* astrometric grid, our aim is to set up a rigorous global solution of astrometric, instrument, and attitude unknowns, complete with the full covariance matrix. The main objective of this paper is to validate the concept of global astrometry with *SIM*. We defer detailed analysis of mission performance until the technical design and schedules are firmly defined.

2. GLOBAL ASTROMETRY WITH *SIM*

The general approach to global astrometry with *SIM* was formulated by Boden (1997). *SIM* will essentially determine the relative angular distances between stars, measured as relative path delays. An elementary observational session that lasts about 1 hr includes delay-line repositioning and fringe integration for a number of objects within one tile, while the baseline orientation and the external path delay is kept stationary. The inevitable drifts of the baseline and the instrument delay line during the time span of one tile are checked by a special regularization process made possible by the external metrology truss and guide interferometer system. It is important in the context of the grid construction that the size of the tile is 15°. Wider angles cannot be directly measured by *SIM*. Tiles are to a large degree independent of each other, inasmuch as they have completely different baseline orientations and delay-line zero points not known a priori to sufficient accuracy. All measurements are made relative to the current regularized baseline, which in turn has to be determined from the same observations. Thus, apart from the astrometric unknowns, the global adjustment will include instrument and baseline parameters.

A typical simulated 5 year grid solution includes five unknown astrometric parameters for each of 1304 grid stars—6520 unknowns in all—one constant path delay offset per tile, and two baseline orientation parameters per tile, which total 154,000 unknowns for the envisaged 48,000 tiles. In addition, up to 26,000 baseline length and field-dependent instrument parameters may need to be fitted. About 186,500 unknowns will have to be solved for, versus the expected 312,000 independent one-dimensional measurements of grid stars, or 240 observations per grid star. Most of these unknowns are baseline orientation and instrument parameters. The system of condition equations is overdetermined by only a factor of 1.67. This is one of the reasons that the grid-average multiplier $m_{\rm astr}$, which relates the average astrometric error for each star (e.g., in position) and the average single measurement error

$$\sigma_{\rm astr} = m_{\rm astr}\, \sigma_{\rm meas} \tag{1}$$

is much larger than the $1/N_{\rm obs}^{1/2}$ that might be expected. Our current simulations yield multipliers about 0.25 for parallaxes, and smaller numbers for positions and proper motions (§ 8). The other reason, which is more important for the understanding of *SIM* astrometry, is the moderate condition of the equations. It stems from the inability of the instrument to measure long arcs on the sky. Since only instantaneous distances shorter than 15° can be measured by *SIM*, large-scale errors (distortions) of astrometric parameters propagate into the solution with larger multipliers than small-scale errors. For example, the dominating error component in grid parallaxes is the zero-point error (§ 9); that is, a constant offset of all parallaxes. The second largest distortion of grid parallaxes is the first zonal harmonic, $n = 1$ and $m = 0$ (Arfken & Weber 1995). This pattern of error propagation accounts for the long-range correlations between astrometric parameters of grid stars.

Although *SIM* will ultimately observe tens of thousands of targets, the fundamental grid that all of the measurements are referenced to consists of approximately 1300 stars that have been specifically chosen for this purpose and have been vetted in a ground-based radial velocity observation campaign. Because of the size of the system, the original algorithm (Boden 1997) developed for its solution was based on an iterative

This content downloaded from 150.135.211.221 on Fri, 18 Nov 2016 23:40:02 UTC
All use subject to http://about.jstor.org/terms

conjugate gradient technique. This made it very difficult to conduct a meaningful covariance analysis, except in an a posteriori manner via a few Monte Carlo mission simulations. Central to the results discussed in this paper is the development of a "deterministic" solution to the problem (i.e., noniterative) that fully exploits the block structure of the regression matrix. It is shown that the least-squares problem can be decoupled into a part that solves only the astrometric parameters (plus ancillary instrument parameters) and a part that solves for the baseline orientation parameters and constant terms. This decoupling is accomplished on a tile-per-tile basis and dramatically reduces the size of the problem, leading to a number of advantages that include improving the speed and accuracy of the solution and the ability to produce the error covariance matrix of the solution.

This latter feature is especially useful since because the grid problem is essentialy linear, many questions can be handled via the error covariance matrix. Questions regarding mission accuracy as a function of observation scenarios, the effect of introducing additional parameters into the solution, understanding zonal errors, etc., are all made more practical because of the availability of the covariance matrix. Furthermore, we can also address the question of how robust the mission is, since it is only one realization of a random distribution.

3. THE *SIM* REGULARIZED DELAY MEASUREMENT

A complete description of the process of the fundamental delay measurement made by the *SIM* instrument can be found in Milman & Turyshev (2000). Here we give a very brief overview of this process, to keep the paper relatively self-contained.

The astrometric observations made by *SIM* require three white-light Michelson interferometer measurements, coupled with various metrology measurements to monitor changes in the distances between a set of fiducials that define the interferometer baseline vectors. The fiducial points correspond to the vertices of high-precision corner cubes. Two of the interferometers lock onto bright guide stars to make precise measurements of changes in the attitude of the instrument. The third interferometer is a science interferometer that makes the delay measurement. This measurement is the projection of its baseline vector onto the unit direction vector of the science target. The external metrology system (there is also an internal metrology system) tracks changes in the three interferometer baseline vectors relative to each other, as well as changes in the baseline lengths.

The delay measurement equation for the science interferometer is

$$d = \langle \boldsymbol{s}, \boldsymbol{b} \rangle + c + \eta, \tag{2}$$

where d is the measured "external" delay (accomplished by white-light fringe measurements and internal metrology measurements), $\boldsymbol{s}$ is the star direction unit vector, $\boldsymbol{b}$ is the interferometer baseline vector, c is the interferometer constant term, η is the noise in the measurement (encompassing both the white-light noise and internal metrology measurement noise), and the angle brackets $\langle \ldots \rangle$ denote the inner product. The astrometric objective is to determine the unknown star direction vector. However, all of the other quantities on the right side of this equation are also unknown. Thus, *SIM* cannot directly measure even the one-dimensional projection of a star vector in a single observation. *SIM* circumvents this difficulty by observing multiple stars with the same baseline vector and constant term within its 15° field of regard:

$$d_i = \langle \boldsymbol{s}_i, \boldsymbol{b} \rangle + c + \eta, \quad i = 1, \ldots, N. \tag{3}$$

SIM then revisits the set of stars within the FOR (the tile) with a new baseline vector and constant term:

$$d_{ij} = \langle \boldsymbol{s}_i, \boldsymbol{b}_j \rangle + c_j + \eta_j, \quad i = 1, \ldots, N, \quad j = 1, \ldots, M. \tag{4}$$

At this point we now have MN equations with $5N + 4M$ unknowns. The astrometric model uniquely defines $\boldsymbol{s}_i$ via mean position coordinates, parallax, and proper motion (i.e., five parameters per star). With enough revisits, eventually $MN \geq 5N + 4M$, so that a well (or over) determined system of equations results.

These equations were formed under the assumption that the baseline vector $\boldsymbol{b}$ is inertially fixed while the measurements are being made. While this assumption is true at the arcsecond level, it is definitely not true at the μas level, which is required for *SIM*; i.e., $\boldsymbol{b}(t)$ is in fact time varying. The *SIM* astrometric analysis presented in Loiseau & Malbet (1996) makes the weaker assumption that there is a fixed but unknown "regularized" baseline vector. This assumption is almost true. In Milman & Turyshev (2000), it is shown that so long as the guide interferometers are locked onto their guide stars and the external metrology subsystem is operating continuously, an estimate of the science baseline vector $\hat{\boldsymbol{b}}$ can be constructed so that

$$\boldsymbol{b}(t) - \hat{\boldsymbol{b}}(t) = \boldsymbol{\delta b} + O(|\boldsymbol{p}||\boldsymbol{\delta x}|), \tag{5}$$

where $\boldsymbol{\delta b}$ is an unknown but *constant* vector, $\boldsymbol{p}$ is an error vector related to uncertainty in the initial parameter conditions of the baseline estimator, and $\boldsymbol{\delta x}$ is the vector of fiducial motion of the optical truss. The parameter vector $\boldsymbol{p}$ includes error in the guide star positions, initial positions of the fiducials, and interferometer zero points (Milman & Turyshev 2000). The magnitudes of $\boldsymbol{p}$ and $\boldsymbol{\delta x}$ are kept very small by imposing requirements on initial instrument knowledge, alignments, and instrument stability.

Introducing the a priori estimates of the star position vectors $\boldsymbol{s}_i^0$ and writing $\boldsymbol{s}_i = \boldsymbol{s}_i^0 + \boldsymbol{\delta s}_i$, where $\boldsymbol{\delta s}_i$ denotes the unknown correction, the astrometric equations more correctly have the

This content downloaded from 150.135.211.221 on Fri, 18 Nov 2016 23:40:02 UTC
All use subject to http://about.jstor.org/terms

form

$$d_i - \langle s_i^0, \hat{b} \rangle = \langle \hat{b}, \delta s_i \rangle + \langle s_i^0, \delta b \rangle + c + \eta. \tag{6}$$

Here $\hat{b}$ and d_i are now time-averaged quantities. This expression is very close to equation (2), but the unknowns are now the correction terms δb and δs_i, and the measurement appearing on the left side above is the so-called "regularized delay" (Boden 1997).

4. EQUATIONS ON A TILE

A tile is defined by a baseline vector b_i^0 and the grid star direction vectors $\{s_{ij}\}$ that are observed within the instrument's field of regard. The regularized delay leads to the equation

$$\delta_{ij} = \langle b_i^0, \delta s_{ij} \rangle + \langle s_{ij}^0, \delta b_i \rangle + c_i. \tag{7}$$

Here s_{ij}^0 denotes the a priori direction values, δs_{ij} and δb_i are the unknown correction vectors to the star positions and baseline vector, respectively, and c_i is the unknown "constant" term. The main objective is to find δs_{ij}. For ease of presentation, we initially model δs as an error in position only. A more proper astrometric model that includes proper motion and parallax is easily incorporated and is discussed at the end of the section.

In the linearized equations, it is assumed that δs_{ij} is a tangent vector to the unit sphere at s_{ij}^0. Let the pair of three–vectors $\{u_{ij}, v_{ij}\}$ be an orthogonal pair of tangent vectors at s_{ij}^0 (Fig. 1). Next we parameterize δb_i by a triad of 3-vectors $\{w_i, y_i, z_i\}$. Because the baseline length is tracked over many tiles by the external metrology subsystem, the parameterization is chosen to easily accommodate this condition. Thus, we take $w_i = b_i^0/|b_i^0|$. One way of generating a global parameterization of all the tangent vectors is to choose a vector e that is not in the set of grid star vectors—for example, the north pole direction—then define

$$u_{ij} = \frac{e \times s_{ij}^0}{|e \times s_{ij}^0|}, \quad v_{ij} = u_{ij} \times s_{ij}^0, \tag{8}$$

and

$$y_i = e \times w_i, \quad z_i = y_i \times w_i. \tag{9}$$

We can rewrite equation (7) in a symmetric fashion by introducing vectors ω_{ij} and ω^i, with

$$\langle \omega_{ij}, s_{ij}^0 \rangle = 0 \quad \text{and} \quad \langle \omega^i, b_i^0 \rangle = 0, \tag{10}$$

so that

$$\delta s_{ij} = \omega_{ij} \times s_{ij}^0 \quad \text{and} \quad \delta b_i = \omega^i \times b_i^0 + \epsilon_i w_i. \tag{11}$$

If the entire 3-vector δB is solved for on each tile, this parameterization appears somewhat superfluous. However, because the baseline length is tracked over many tiles by the external metrology subsystem, a nonlinear constraint on the length of the baseline is introduced. The ϵ term is related to the linearized form of the baseline length.

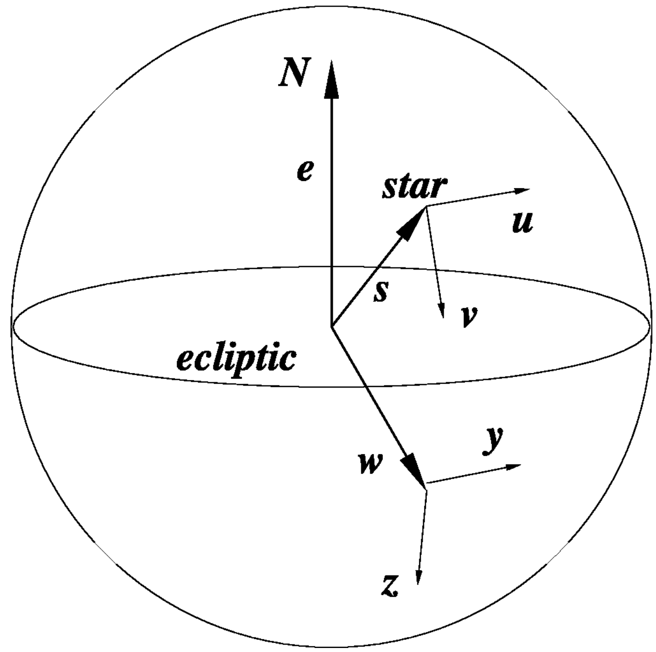

Fig. 1.—Vectors in equations on a tile.

Thus,

$$\delta_{ij} = \langle b_i^0 \times s_{ij}^0, \omega^i \rangle - \langle b_i^0 \times s_{ij}^0, \omega_{ij} \rangle + \epsilon_i \langle w_i, s_{ij}^0 \rangle + c_i. \tag{12}$$

Note the deficiency in the equations due to global rotations; i.e., if we set

$$\omega_{ij} = \omega^i = \gamma, \tag{13}$$

for some fixed $\gamma \in R^3$ and for all i and j, and set $c_i = \epsilon_i = 0$ in equation (12), then the right side is zero.

Since it only takes two parameters each to characterize ω_{ij} and ω^i, because of the constraints equation (10), we do so here by writing $\omega_{ij} = \alpha_{ij} u_{ij} + \beta_{ij} v_{ij}$ and $\omega^i = g_i y_i + h_i z_i$. Hence,

$$\begin{aligned} \delta_{ij} &= \langle b_i^0 \times s_{ij}^0, \omega^i \rangle - \langle b_i^0 \times s_{ij}^0, \omega_{ij} \rangle + \epsilon_i \langle w_i, s_{ij}^0 \rangle + c_i \\ &= g_i \langle b_i^0 \times s_{ij}^0, y_i \rangle + h_i \langle b_i^0 \times s_{ij}^0, z_i \rangle + \epsilon_i \langle w_i, s_{ij}^0 \rangle \\ &\quad + c_i - \alpha_{ij} \langle b_i^0 \times s_{ij}^0, u_{ij} \rangle - \beta_{ij} \langle b_i^0 \times s_{ij}^0, v_{ij} \rangle, \end{aligned} \tag{14}$$

with unknown parameters g_i, h_i, α_{ij}, β_{ij}, c_i, and ϵ_i. In what follows, we neglect the contribution of the baseline length pa-

This content downloaded from 150.135.211.221 on Fri, 18 Nov 2016 23:40:02 UTC
All use subject to http://about.jstor.org/terms

rameter ϵ_i. Ultimately it is re-introduced in a more general fashion as an instrument parameter in § 5.

We assume there are N_i grid stars in the tile and define the $N_i \times 3$ matrix B_i, whose jth row is

$$B_{ij} = [\langle \boldsymbol{b}_i^0 \times \boldsymbol{s}_{ij}^0, \boldsymbol{y}_i \rangle \langle \boldsymbol{b}_i^0 \times \boldsymbol{s}_{ij}^0, \boldsymbol{z}_i \rangle 1]. \quad (15)$$

We also define the $N_i \times 2N_i$ matrix S_i with a jth row

$$S_{ij} = -[0_{1,\,2(j-1)} \langle \boldsymbol{b}_i^0 \times \boldsymbol{s}_{ij}^0, \boldsymbol{u}_{ij} \rangle \langle \boldsymbol{b}_i^0 \times \boldsymbol{s}_{ij}^0, \boldsymbol{v}_{ij} \rangle 0_{1,\,2(N_i-1)}], \quad (16)$$

where $0_{p,\,q}$ denotes the $p \times q$ zero matrix. The system of equations can now be written as

$$B_i X_i + S_i Y_i = \delta_i, \quad (17)$$

where

$$X_i = \begin{bmatrix} g_i \\ h_i \\ c_i \end{bmatrix}, \quad Y_i = \begin{bmatrix} \alpha_{i1} \\ \beta_{i1} \\ \vdots \\ \alpha_{iN_i} \\ \beta_{iN_i} \end{bmatrix}, \text{ and } \delta_i = \begin{bmatrix} \delta_{i1} \\ \vdots \\ \delta_{iN_i} \end{bmatrix}. \quad (18)$$

In Appendix A, it is shown that B_i has full rank ($\mathrm{rank} = 3$). Therefore, it can be assumed without loss of generality (or achieved by a permutation of rows) that rows four through N_i can be written as a linear combination of the first three rows. Thus, by performing elementary row operations in equation (17), we can eliminate the instrument variables g_i, h_i, and c_i in rows 4 through N_i of equation (17).

Another way of accomplishing this is to use *QR* factorization (Golub & Van Loan 1989)

$$B_i = Q_i \begin{bmatrix} R_i \\ 0_{N_i-3,\,3} \end{bmatrix}, \quad (19)$$

where Q_i is an $N_i \times N_i$ orthogonal matrix and R_i is a 3×3 invertible upper triangular matrix. This has the advantage of maintaining the integrity of the least-squares problem associated with the equation (17) system. Multiplying equation (17) by Q_i^T yields the pair of equations

$$R_i X_i + \tilde{S}_i^+ Y_i = \tilde{\delta}_i^+, \quad (20)$$

$$\tilde{S}_i^- Y_i = \tilde{\delta}_i^-, \quad (21)$$

where $\tilde{S}_i^+$ is a $3 \times 2N_i$ matrix formed from the top three rows of $Q^T S_i$, and $\tilde{S}_i^-$ is an $(N_i - 3) \times 2N_i$ matrix formed from the remaining bottom rows of $Q^T S_i$. Vectors $\tilde{\boldsymbol{\delta}}_i^{\pm}$ are analogously defined.

Including proper motion and parallax into the formulation is straightforward. The model for the perturbation of the star position as a tangent vector is now time varying:

$$\boldsymbol{\delta s}(t) = \boldsymbol{\omega} \times \boldsymbol{s}^0 + t\boldsymbol{\omega}^p \times \boldsymbol{s}^0 + \pi \boldsymbol{q}(t), \quad (22)$$

where $\boldsymbol{\omega}^p$ accounts for the proper motion (and again $\langle \boldsymbol{\omega}^p, \boldsymbol{s}^0 \rangle = 0$), π is the parallax, and $\boldsymbol{q}(t)$ is the time-varying tangent vector related to the orbital position $\phi(t)$ of the interferometer relative to the solar system barycenter:

$$\boldsymbol{q}(t) = \langle \boldsymbol{s}^0, \phi(t) \rangle \boldsymbol{s}^0 - \phi(t). \quad (23)$$

Thus, equation (12) becomes

$$\begin{aligned} \delta_{ij} = {} & \langle \boldsymbol{b}_i^0 \times \boldsymbol{s}_{ij}^0, \boldsymbol{\omega}^i \rangle - \langle \boldsymbol{b}_i^0 \times \boldsymbol{s}_{ij}^0, \boldsymbol{\omega}_{ij} \rangle \\ & - \langle t\boldsymbol{b}_i^0 \times \boldsymbol{s}_{ij}^0, \boldsymbol{\omega}_{ij}^p \rangle + \langle \boldsymbol{b}_i^0, \boldsymbol{q}_{ij}(t) \rangle \pi_{ij} \\ & + \epsilon_i \langle \boldsymbol{w}_i, \boldsymbol{s}_{ij}^0 \rangle + c_{i.} \end{aligned} \quad (24)$$

Now the astrometric vector Y in equation (17) is extended to include proper motion and parallax:

$$Y = \begin{bmatrix} Y_{\mathrm{pos}} \\ Y_{\mathrm{pm}} \\ Y_{\mathrm{par}} \end{bmatrix}, \quad (25)$$

with the obvious interpretation of the subscripts.

Note also that the size of the null space of the grid solution increases to six, since by choosing $\boldsymbol{\omega}_{ij}^p = \boldsymbol{\gamma}$, for some fixed 3-vector $\boldsymbol{\gamma}$ and all i, j, and setting $\boldsymbol{\omega}^i = t_i \boldsymbol{\gamma}$, where t_i is the time of the ith tile observation (assuming stellar dynamics are negligible over the observation of a tile; approximately 1 hr), and setting all other variables to zero, we find a solution to the global equations. If a priori proper motions and parallaxes are introduced, the variables above should be interpreted as corrections to these values.

5. EQUATIONS ON THE GRID

To introduce the algorithm as it will be applied to the entire grid, it is necessary to make a change in the indexing notation for the star position correction parameters, since an individual star will appear in multiple tiles, while each baseline uniquely defines the tile. We assume there are a total of N stars in the grid. Now we let Y denote the set of correction parameters for the entire grid of stars so that Y has length $5N$. Then equation (21) becomes

$$R_i X_i + \tilde{S}_i^+ H_i Y = \tilde{\delta}_i^+, \quad (26)$$

$$\tilde{S}_i^- H_i Y = \tilde{\delta}_i^-, \quad (27)$$

where H_i is an $5N_i \times 5N$ matrix that picks off the appropriate components of the $5N$-vector Y. Next, we define $S_i^{\pm} \equiv \tilde{S}_i^{\pm} H_i$

This content downloaded from 150.135.211.221 on Fri, 18 Nov 2016 23:40:02 UTC
All use subject to http://about.jstor.org/terms

and suppose there are a total of M tiles. Then the system of equations has the block form

$$\begin{bmatrix} R_1 & \cdots & & S_1^+ \\ & \ddots & & \\ 0 & \cdots & R_M & S_M^+ \\ 0 & \cdots & & S_1^- \\ \cdots & & & \vdots \\ & & \cdots & S_M^+ \end{bmatrix} \begin{bmatrix} X \\ Y \end{bmatrix} = \begin{bmatrix} \delta^+ \\ \delta^- \end{bmatrix}, \tag{28}$$

where

$$X = \begin{bmatrix} X_1 \\ \vdots \\ X_M \end{bmatrix}. \tag{29}$$

More compactly, we can write

$$G \begin{bmatrix} X \\ Y \end{bmatrix} = \begin{bmatrix} \delta^+ \\ \delta^- \end{bmatrix}, \quad G = \begin{bmatrix} R & S^+ \\ 0 & S^- \end{bmatrix}. \tag{30}$$

It is important to note here that the reduction from the original set of grid equations to the system above is accomplished using only *orthogonal* transformations. Specifically, if each Q_i acting on a single tile is extended to the entire set of grid equations via appending the identity, this extension is also an orthogonal matrix. Furthermore, the partitioning of the astrometric and instrument parameters uses permutation matrices, which are also orthogonal. Thus, the entire reduction is accomplished by multiplications of these extended matrices and permutation matrices. The result of the entire product is then also an orthogonal matrix. Hence, the original least-squares problem is preserved; i.e., if the original problem is

$$\min_x |Ax - b|^2, \tag{31}$$

then the transformed problem

$$\min_x |QAx - Qb|^2 \tag{32}$$

has the same solution, since Q preserves norms; i.e., $|Qy| = |y|$ for any matrix y.

The baseline vector orientation terms and constant terms are stored in the vector X, while the astrometric parameters are stored in Y. The length of X is $3 \times M$ and the length of Y is $5 \times N$. Note that for the grid problem, $3 \times M \gg 5 \times N$.

Writing G for the matrix on the left above, the least-squares problem is

$$\min_{X,Y} \left| G \begin{bmatrix} X \\ Y \end{bmatrix} - \begin{bmatrix} \delta^+ \\ \delta^- \end{bmatrix} \right|^2$$
$$= \min_{X,Y} \{|RX + S^+Y - \delta^+|^2 + |S^-Y - \delta^-|^2\}. \tag{33}$$

But since R is invertible (it is composed of M blocks of 3×3 invertible matrices), for any choice of Y_0,

$$\min_X |RX + S^+Y_0 - \delta^+|^2 = 0 \tag{34}$$

is obtained by choosing

$$X = R^{-1}[\delta^+ - S^+Y_0]. \tag{35}$$

Thus, equation (33) is equivalent to the decoupled set of problems

$$\min_Y |S^- Y - \delta^-|^2, \tag{36}$$

followed by

$$\min_X |RX + S^+Y^* - \delta^+|^2, \tag{37}$$

where Y^* is the solution to equation (36). Thus, we can solve for the astrometric parameters without ever determining the baseline parameters.

The reduction of the original least-squares problem to equation (36) is quite inexpensive when using sparse-matrix multiplication. Each tile requires an $N_i \times N_i$ by $N_i \times 5N_i$ matrix multiplication. The back-substitution to determine X once Y has been solved for is also inexpensive. The major computational burden is to solve the least-squares problem of equation (36).

As noted earlier, the grid problem is rank deficient in general because of the existence of global rotations of the entire grid and baseline vectors that lead to null solutions. One way of circumventing this difficulty is to introduce pinned objects (see Swartz 2003). Doing so removes the rank deficiency in G. The invertibility of R implies that S^- must be full rank as well. An alternative approach to eliminating the rank deficiency is to explicitly remove the null space. Once the problem is reduced to a full-rank problem, standard techniques (e.g., QR factorization, normal equations) can be used to solve the least-squares problem.

6. EXTENSIONS OF PARAMETERS

We present an approach that is the most straightforward extension of the existing algorithm. This approach entails appending the new instrument parameters to the set of astrometric parameters, thus allowing the removal of the baseline orien-

This content downloaded from 150.135.211.221 on Fri, 18 Nov 2016 23:40:02 UTC
All use subject to http://about.jstor.org/terms

tation and constant term parameters on a tile-per-tile basis, just as before. As an important example, suppose v contains the baseline length parameters that are updated on a multi-tile basis (e.g., every 10 tiles or 20 tiles, or perhaps some combination). To accommodate this situation, we introduce the vector of unknown baseline length parameters as $\boldsymbol{v} = (\epsilon_1, \ldots, \epsilon_M)$, where M represents the total number of different baseline lengths that need to be estimated. On a given tile (say, the ith tile), the delay measurement equation includes the baseline length term expression

$$\epsilon_k \langle \boldsymbol{b}_i / |\boldsymbol{b}_i|, \boldsymbol{s}_{ij} \rangle, \quad j = 1, \ldots, N(i), \tag{38}$$

where $\boldsymbol{b}_i$ is the a priori baseline vector and $\boldsymbol{s}_{ij}$ represents the a priori stellar position vectors for the targets in the tile. The scalar ϵ_k is the unknown parameter that represents the difference between the a priori baseline length and the true length. Other parameters can be introduced in a similar fashion.

So again we have equation (30), but now the Y vector is extended as

$$Y_{\text{ext}} = \begin{bmatrix} Y \\ v \end{bmatrix}, \tag{39}$$

where v is the vector of instrument parameters. The submatrices $S^{\pm}$ in equation (30) are extended as

$$S_{\text{ext}}^{\pm} = [S^{\pm} \quad V^{\pm}], \tag{40}$$

where $V^{\pm}$ represent the reduced regression matrices for the instrument parameters. The system of equations now takes the form

$$G \begin{bmatrix} \boldsymbol{X} \\ Y_{\text{ext}} \end{bmatrix} = \delta, \qquad G = [R \quad S_{\text{ext}}^{+} \;\; 0 \;\; S_{\text{ext}}^{-}]. \tag{41}$$

A necessary assumption at this point is that if the vectors $\boldsymbol{U}_1, \ldots, \boldsymbol{U}_r$ span the null space of S^-, then the set of vectors

$$\left\{ \begin{bmatrix} \boldsymbol{U}_i \\ 0 \end{bmatrix} \right\}_{i=1,r} \tag{42}$$

span the null space of S_{ext}. If this condition is not met, the delay data would not be able to discriminate between an instrument parameter vector and some linear combination of astrometric parameters, and the astrometry would not be recoverable.

7. SOLUTION OF LINEARIZED SYSTEM AND CALCULATION OF COVARIANCE MATRIX

With a slight abuse of notation, the least-squares problem we are now solving is

$$\min_{Y_{\text{ext}}} |S_{\text{ext}}^{-} Y_{\text{ext}} - \delta|^2, \tag{43}$$

where δ is the QR-processed regularized delay measurement. At this point, S_{ext}^{-} still contains a null space, so it is necessary to remove 6 degrees of freedom to ensure that it has maximal column rank.

Now assume that 6 degrees of freedom have been removed from S^- and call this resulting full-rank matrix S_U. For notational convenience, we also write V for V^- in the sequel. We discuss solving this system from the perspective of using the normal equations. As an intermediate step, the covariance matrix is also derived. From equation (40), we see that the covariance matrix for the astrometric and auxiliary instrument parameters is X^{-1}, where

$$X = \begin{bmatrix} S_U^T S_U & S_U^T V \\ V^T S_U & V^T V \end{bmatrix}. \tag{44}$$

If V has many columns, X can be inverted via a standard partitioning technique (Halmos 1982). That is, for an invertible matrix K,

$$K = \begin{bmatrix} A & B \\ C & D \end{bmatrix}, \tag{45}$$

K^{-1} is obtained as (assuming all of the inverses below exist)

$$K^{-1} = \begin{bmatrix} E^{-1} & -E^{-1}BD^{-1} \\ -D^{-1}CE^{-1} & D^{-1}CE^{-1}BD^{-1} + D^{-1} \end{bmatrix}, \tag{46}$$

where

$$E = A - BD^{-1}C. \tag{47}$$

Making the appropriate substitutions, we find that

$$\begin{aligned} E &= A - BD^{-1}C \\ &= S_U^T S_U - S_U^T V (V^T V)^{-1} V^T S_U \\ &= S_U^T S_U - S_U^T P_V S_U, \end{aligned} \tag{48}$$

where P_V denotes the orthogonal projection onto the range of V. [As is readily verified, $P_V = V(V^T V)^{-1} V^T$.] The notation E^{-1} is the covariance matrix for the astrometric parameters, and the form of E above reveals how introducing additional parameters affects the astrometric accuracy.

In general, E^{-1} is dependent on how the degeneracy in the problem is eliminated. Let E_{null}^{-1} denote the covariance matrix that results when the null space is specifically removed, and let E^{-1} denote the resulting covariance matrix obtained by any other means of removing the rank deficiency of the problem

This content downloaded from 150.135.211.221 on Fri, 18 Nov 2016 23:40:02 UTC
All use subject to http://about.jstor.org/terms

(e.g., pinning objects). It can then be shown that (Milman 2003)

$$\mathrm{tr}(E_{\mathrm{null}}^{-1}) = \mathrm{tr}(E^{-1}) - \sum_i U_i^T E^{-1} U_i, \tag{49}$$

where the U_i are an orthonormal set that span the null space. Thus, the smallest computed error is obtained by specifically removing the null vectors. This relationship is important to the *SIM* project, because the standard metric that is used to characterize mission accuracy is the average error over the grid. This error is captured by the covariance matrix via $[\mathrm{tr}(E^{-1})/N]^{1/2}$, where N denotes the number of astrometric parameters. Prior to the availability of the covariance matrix, simulations were performed, and with each simulation a global rotation of the grid solution was made to minimize the error as measured by "truth" to obtain a reasonable estimate of the mission accuracy.

Obtaining the astrometric parameters from the (*QR*-factorized) regularized delay measurements δ can also be done in block form. Specifically, noting that the astrometric and instrument parameters are derived via

$$\begin{bmatrix} \hat{Y} \\ \hat{v} \end{bmatrix} = X^{-1} \begin{bmatrix} S_U^T \delta \\ V^T \delta \end{bmatrix}, \tag{50}$$

from equations (46) and (48), we get

$$\hat{Y} = E^{-1} S_U^T \delta - E^{-1} S_U^T V (V^T V)^{-1} V^T \delta \tag{51}$$

$$= E^{-1} S_U^T \delta - E^{-1} S_U^T P_V \delta. \tag{52}$$

As stated above, the grid-reduction equations are in general nonlinear. However, for the envisaged a priori knowledge of the astrometric parameters, the linearization presented is a very accurate representation; 100 mas class errors lead to sub-μas errors as a result of the linearization. Furthermore, the rest of the system of equations is linear, except for the constraint on the baseline length parameter. In fact, if this parameter were updated on each tile, the system would be linear. But even with larger a priori knowledge errors and the baseline length constraint, a single iteration of the solution generally converges to sub-μas accuracy.

8. COVARIANCE ANALYSIS AND THE GRID ACCURACY

Construction of a rigid, high-accuracy astrometric grid is one of the main objectives of the *SIM* mission. The *SIM* grid is a system of astrometric parameters of a limited number of evenly distributed stars (currently 1304), selected as the most likely stable, nonbinary, and sufficiently bright stars. This system defines a global (possibly rotating) reference frame, with respect to which all other astrometric measurements on science target objects will be made. Since the science value of the grid stars is relatively low, the grid astrometry is an ancillary (but essential) data product of the mission. Its practical purpose is to achieve a consistent and accurate solution for baseline orientation and calibration unknowns, which will be used in the processing of target object observations. As stated in § 1, *SIM* is not able to determine its orientation to the required accuracy by any other means but its own observations and subsequent astrometric reductions, which may take years to perform.

Preliminary analysis of the wide-angle astrometric processing (the basic mode of absolute astrometry with *SIM*) indicates that the best mission performance achievable for science targets is close to the ultimate grid accuracy. This drives the central mission requirement of (currently) 4 μas accuracy for grid parallaxes. If this performance goal is achieved, science star parallaxes, positions, and proper motions per tangential coordinate can be obtained to similar or slightly better accuracy. We discuss below the numerical simulations of global grid solutions and the conditions under which the goal requirement can be met.

The grid reductions, as outlined in the previous section, is a direct, one-step global least-squares adjustment of global unknowns that falls into three major categories: (1) astrometric parameters, (2) baseline orientation parameters, and (3) instrument calibration parameters. The first group is the smallest one, consisting of five parameters (or seven, if accelerations of proper motions are required) per star, thus amounting to about 6500 unknowns. The number in the second group is the number of tiles during a 5 year mission times two coordinates of the baseline vector, or approximately 96,000. The third group includes constant path delay offsets (one for each tile; about 48,000 in all) and a number of field-dependent terms that depends on the time variability of the calibration function. We consider a generalized calibration model in which field-dependent corrections are represented by orthogonal Zernike polynomials, but the baseline length is treated separately. The total number of instrument calibration parameters we have attempted to solve is up to 100,000.

The astrometric multipliers (eq. [1]) that link the mission-average accuracy to the mean single-measurement precision σ_0 are defined via the trace of the astrometric block of the full covariance matrix:

$$m_{\mathrm{astr}} = \sqrt{\mathrm{tr}(C_A)/N}, \tag{53}$$

where N is the number of fitted parameters. In a similar fashion, by extracting corresponding submatrices, the accuracy multipliers for positions, parallaxes, and proper motions are defined. The astrometric part of the covariance matrix is derived from equation (49). Table 1 gives the average multipliers determined in full-scale grid simulations. Using an estimated 10 μas the single-measurement error on a grid star,[3] mission-average par-

[3] This quantity is defined as the quotient of the delay measurement error and baseline length.

This content downloaded from 150.135.211.221 on Fri, 18 Nov 2016 23:40:02 UTC
All use subject to http://about.jstor.org/terms

TABLE 1
MISSION-AVERAGE GRID MULTIPLIERS (EQS. [1] AND [53]) FOR POSITIONS, PARALLAXES, PROPER MOTIONS AND BASELINE LENGTH (BLL)

Calibration Interval Tiles	m_{pos}	m_{par}	m_{pm}	m_{BLL}
480	0.210	0.243	0.146	0.0323
100	0.263	0.259	0.183	0.0837
48	0.291	0.270	0.202	0.1212
30	0.321	0.292	0.223	0.1601

allax accuracies of 2.4–2.9 μas are predicted. Although this is much better than the goal of 4 μas, this standard error does not include other sources of error, such as the effects of metrology drift, second-order error coupling, field-dependent errors, and others. Physical error models predict that the goal performance can be achieved if the astrometric multipliers stay within 0.25. Hence, our simulations confirm that the desired astrometric accuracy is attainable with the current design of *SIM* if the frequency of calibration solutions is sufficiently low. In these simulations, we assumed for simplicity that the calibration function of the instrument, represented by the baseline length (BLL) parameter and Zernike terms to fourth order, is fairly constant over a certain interval of observation (termed "calibration interval" in Table 1); e.g., 480 consecutive tiles. Thus, the mission time is partitioned into equal segments, and an independent set of calibration parameters is determined for each segment. Details of an extensive *SIM* mission simulation tool can be found in Murphy & Meier (2004).

It turns out that the BLL parameter is a special calibration parameter in the grid reductions. It is similar to the scale parameter in photographic plate astrometry. The main difference between the two is that the former is one-dimensional (since only distances projected onto the baseline vector matter), while the latter is two-dimensional. A small change in BLL will make all the measured distances expand or shrink proportionally with respect to a common origin in the FOR, defined by the true normal to the baseline vector. In photographic astrometry, the scale factor is a parameter whose determination lies with the so-called closure condition. If the entire sphere is covered with plates with some overlap, or is at least a round strip along a great circle, an error in the assumed scale will make the total estimated length differ from 2π. Since a considerable number of plates are used in this condition, the astrometric error grows as the overlap solution progresses around the sphere.

The presence of the scale parameter in the grid adjustment generally does not make the condition equations rank-deficient. Indeed, consider a tile with a pair of grid stars at certain projected distances x_1 and x_2 from the center of the tile. The observable difference in regularized delays for this pair will be $d = B(\sin x_1 - \sin x_2) \approx B(x_1 - x_2 + x_2^3/6 - x_1^3/6)$, where B is the baseline length. Placing another tile with the center shifted by some amount along the same projected baseline direction, the delay difference will change due to the third and higher order terms. That change will be proportional to the actual baseline length, hence the latter will be determinable. Alternatively, the tile could be re-observed with a baseline direction slightly tilted by a known amount, changing the projected distance difference. Thus, it is important for a self-calibrating interferometer that the same group of stars is measured in several overlapping tiles at different baseline orientations.

Even though rank deficiency can be avoided just by using a pair of overlapping tiles, it is hard to ensure a good condition for the equations, since translation or tilt of the tile causes a change in relative delays that is fairly similar to the linear dependence on BLL (in other words, $\sin x \approx x$ at small x). Therefore, solving for BLL and baseline orientation simultaneously on a small set of overlapping tiles is an ill-conditioned problem. For example, a dilation of a finite field is hard to discriminate from an increase in the BLL. To build up a two-dimensional lacework of an astrometric grid with the relatively small FOR of *SIM*, a fairly complete coverage of the sky is necessary. Conversely, how often the BLL and other field-dependent parameters have to be redetermined during the mission establishes the ultimate grid accuracy and the BLL accuracy (Table 1), which is important for the subsequent wide-angle and narrow-angle data reductions. The ultimate success of the mission hinges on how stable the interferometer can be made on orbit, rather than on exact a priori knowledge of instrument characteristics.

Thus far, we have considered only the diagonal elements of the covariance matrix of the grid solution, which provide variance estimates of adjusted parameters. We note that even though the baseline orientation unknowns are eliminated from the design matrix by *QR* factorization, the available covariances are correct for the full-rank problem. Furthermore, the off-diagonal elements of the astrometric part of the matrix contain important information about star-to-star correlations of the solution. This is exactly the kind of information that is missing in the *Hipparcos* solution, which does not allow us to correctly compute the error of the Pleiades parallax, for example, as discussed in § 1. Understanding the astrometric correlations is important for the correct interpretation of *SIM* data. The character of global astrometry with *SIM* gives rise to significant correlations between the parameters of grid stars in extended areas. Such correlations propagate into the wide-angle reductions undiminished. They must be taken into account in astrophysical studies concerning sets of stars, for example, in investigations of the dynamics of particular parts of the Galaxy where large numbers of parallaxes and proper motions are utilized. Figure 2 depicts the proper-motion residuals "computed minus true" for grid stars in an area around the Galactic center, in a typical simulation. Although the pattern of the errors is completely random from simulation to simulation, for one particular mission it looks like a systematic error, in that most of the residual vectors are pointing the same way. The origin of

This content downloaded from 150.135.211.221 on Fri, 18 Nov 2016 23:40:02 UTC
All use subject to http://about.jstor.org/terms

the pattern, somewhat surprisingly, is in the uncorrelated accidental errors of individual delay measurements. The pattern is not predictable for a real *SIM* mission, but the uncertainties and correlations of any statistics based on these data are exactly quantified by the covariance matrix.

Even more pronounced correlation effects were found for grid parallaxes. Our simulations show that almost all correlations between individual parallaxes all over the sky are positive. That is to say, almost all grid parallaxes will have errors of the same sign with respect to true parallaxes. This property is directly related to the error of the parallax zero point. More insight into the propagation of zero-point and other large-scale errors can be gained through a spherical harmonic decomposition analysis.

9. SPHERICAL HARMONIC ANALYSIS

Spherical harmonic analysis of global astrometric error distributions gives insight into the propagation of errors and a better understanding of the ultimate quality of the mission astrometric solution (Makarov 1998). It helps to create a comprehensible picture of how accidental (and possibly systematic) errors in the raw observational data are transformed into the imprecisions of positions, parallaxes, and proper motions. For simplicity, we consider the parallax error distribution, although the same method can be applied to proper motion and position components. Spherical harmonics are expressed via Legendre polynomials P_n^m and Fourier harmonics in longitude by

$$\mathrm{Re}(Y_{nm}) = \sqrt{\frac{2n+1}{2\pi}\frac{(n-m)!}{(n+m)!}}P_n^m(\cos\theta)\cos m\phi,$$
$$n = 0, 1, \ldots;\ m = 0, 1, \ldots, n,$$
$$\mathrm{Im}(Y_{nm}) = \sqrt{\frac{2n+1}{2\pi}\frac{(n-m)!}{(n+m)!}}P_n^m(\cos\theta)\sin m\phi,$$
$$n = 0, 1, \ldots;\ m = 0, 1, \ldots, n, \tag{54}$$

where $\theta \in [0, \pi]$ is the polar distance in the coordinate system of choice (the ecliptic system in this paper) and $\phi \in [0, 2\pi]$ is the longitude. The spherical functions are called tesseral functions at $n \neq m$ and $m \neq 0$, sectorial harmonics at $n = m$, and zonal harmonics at $m = 0$. The spherical functions are orthonormal in the sense that for the inner product of two functions f and h,

$$(f, h) = \int_0^{2\pi} d\phi \int_0^{\pi} \bar{f}(\theta, \phi)h(\theta, \phi)\sin\theta d\theta \tag{55}$$

$$= \begin{cases} 0, & f \neq h \\ 1, & f = h \end{cases}, \tag{56}$$

Let δ_Π be the column vector of parallax errors δ_{Π_i}, $i = 1, 2, \ldots, N$ of N grid stars in the final grid catalog (i.e., $\delta_{\Pi_i} = \Pi_i - \Pi_{\mathrm{true},\, i}$). Each of the individual errors can be uniquely approximated via J spherical functions:

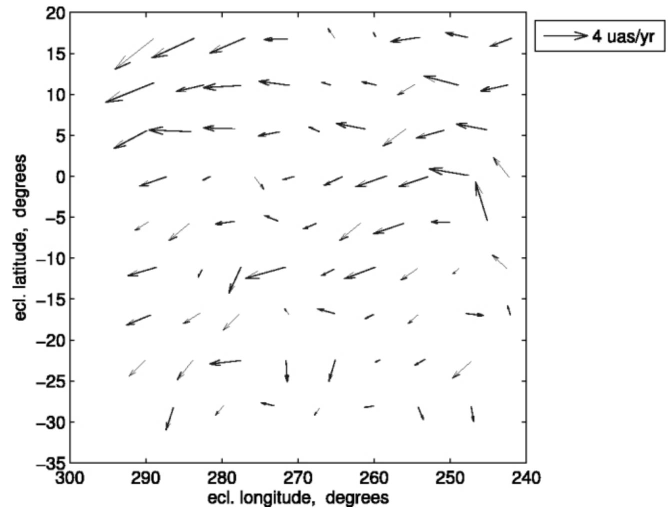

FIG. 2.—Simulated absolute errors of proper motions of grid stars around the direction to the Galactic center in a single mission realization.

$$\delta_{\Pi_i} \approx \sum_{j=1}^{J} a_j Y_j(\phi_i, \theta_i), \tag{57}$$

where the index j counts possible combinations (n, m), starting with low degrees and orders. Hence, if we define the matrix Y to be

$$Y = \begin{bmatrix} Y_{11} & Y_{12} & \ldots & Y_{1J} \\ \ldots & & & \\ Y_{N1} & Y_{N2} & \ldots & Y_{NJ} \end{bmatrix} \tag{58}$$

and the vector a to be the column vector of $a_1, a_2, \ldots, a_J$, then

$$\tilde{\delta}_\Pi \approx Y a. \tag{59}$$

It can be proven that if the columns of Y are orthogonal and $J = N$ (that is, the number of different spherical harmonics in the expansion in equation (57) equals the number of data points on the sphere), then the exact equality is achieved:

$$\delta_\Pi = Y a \tag{60}$$

and the coefficients a_i can be computed by

$$a = Y^{\mathrm{T}}\delta_\Pi. \tag{61}$$

For a uniform distribution of a large number of grid stars on the sphere, the sampled spherical harmonics Y_j are approximately orthogonal. Slight nonregularities in the distribution of

This content downloaded from 150.135.211.221 on Fri, 18 Nov 2016 23:40:02 UTC
All use subject to http://about.jstor.org/terms

grid stars on the sphere will make the sampled harmonics slightly nonorthogonal, especially at high degrees and orders (when j is closer to N). But for any set of stars, the harmonics can be made strictly orthogonal by the Gram-Scmidt algorithm, for example.

We investigate the covariances of parallax errors:

$$\mathrm{Cov}\,(\delta_\Pi) = E(Y\,a\,a^\mathrm{T}\,Y^\mathrm{T}) = Y\ \mathrm{Cov}\,(a)\,Y^\mathrm{T}. \qquad (62)$$

It becomes obvious that the diagonal elements of Cov (a), which itself is nearly diagonal, are approximately the singular values of Cov (δ_Π), and the columns of Y are its eigenvectors. The largest singular value corresponds to the eigenvector (discrete spherical harmonic) in which the largest propagation of errors takes place.

Using simulated data files for a 5 year mission (generated by Swartz 2003) and a prototype grid solution code, we computed astrometric solutions, covariance matrices, and spherical harmonic decompositions for a provisional observing schedule, assuming 1304 grid stars evenly distributed across the sky. Only uncorrelated random errors in delay measurements were considered, and all observations were assumed to have the same weight. The observing schedule is a winding pattern of overlapping tiles starting at the south ecliptic pole and going in small circles toward the north pole, jumping over the Sun exclusion zone. The Sun exclusion zone encompasses the area of the sky where no *SIM* observations are possible, currently a circle of 60° radius centered on the Sun. Each tile contained six to seven grid stars, and each star was observed about 250 times. Only astrometric parameters, baseline orientations, constant terms, and baseline lengths were solved for, the latter once per 480 consecutive tiles. From the resulting astrometric part of the covariance matrix (5 × 1304 on a side), we extracted the block corresponding to the 1304 fitted parallaxes. By using equation (61), the variance of the coefficient $\boldsymbol{a}_j$ can be directly computed for any sampled spherical harmonic Y_j. Figure 3 shows with circles the resulting standard deviations (square roots of the variances) for the first 289 spherical harmonics, beginning with the zeroth-order harmonic, which is a constant unity. A single measurement error of 15 μas (1 σ) was assumed.

This plot shows the important property of the parallaxes obtained with *SIM*. The dominant error term in grid parallaxes (and subsequently in science target parallaxes) is the constant error on the sphere, which in astrometry is often called the zero-point error (Hanson 1980; Arenou et al. 1995). This term is so much larger than the other position-dependent terms that quite likely, the external errors $\delta\Pi_i$ will all have the same sign. As the standard deviations drop off very rapidly with increasing order, the pattern resembles a "red spectrum" of noise. The overall distribution of parallax error is chiefly a constant shift plus some random large-scale distortions, with a small addition of high-frequency noise from the numerous high-order spherical harmonics. Subsequently, most of the individual parallaxes are expected to be positively correlated. This must be taken into account in any astrophysical study related to ensembles of stars. On the other hand, the accuracy of relative astrometric parameters may be better than the accuracy of their combination. For example, variances of relative proper motions of nearby stars can be significantly smaller than the sum of individual variances, due to positive correlations. Numerical simulations show that the zero-point error decreases by 60% if 38 optically bright quasars are included in the grid and observed to the same precision as regular grid stars.

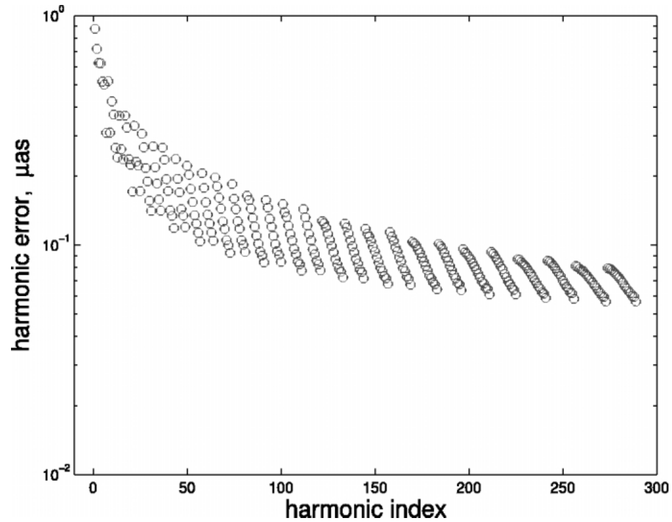

FIG. 3.—Standard deviations of the spherical harmonic coefficients representing the global parallax error distribution, computed with the grid code. A single delay measurement error of 15 μas was assumed. The indexing of spherical harmonics is described in the text.

For a single mission, the distribution $\delta\Pi_i$ on the sphere is a random vector if the measurement noise is random and uncorrelated. But the distribution of parallax covariance Cov (δ_Π) is a deterministic matrix that is defined by the measurement covariance matrix and the observing schedule. By picking off one of the variances in Cov (a) and performing the multiplications in equation (62), the distribution of errors propagating through the corresponding spherical harmonic can be reconstructed. Any desirable part of Cov (a) can be computed by inverting equation (62). As we already know, the error distribution is dominated by low-order harmonics for *SIM* (Fig. 3). Therefore, the general distribution will be quite close to the pattern produced by a finite number of low-order harmonics. This pattern is useful for the investigation of the uniformity of the error distribution, as governed by the adopted observing scenario. The pattern of parallax error distribution in Figure 4, computed for the first 122 harmonics (up to order 10), reveals that the ultimate accuracy will not be uniform across the sky, despite the quite uniform distribution of grid stars and equal single-measurement precision for all stars. Parallaxes near the poles are significantly more accurate than around the ecliptic. A finer pattern of accuracy distribution emerges in the near-

This content downloaded from 150.135.211.221 on Fri, 18 Nov 2016 23:40:02 UTC
All use subject to http://about.jstor.org/terms

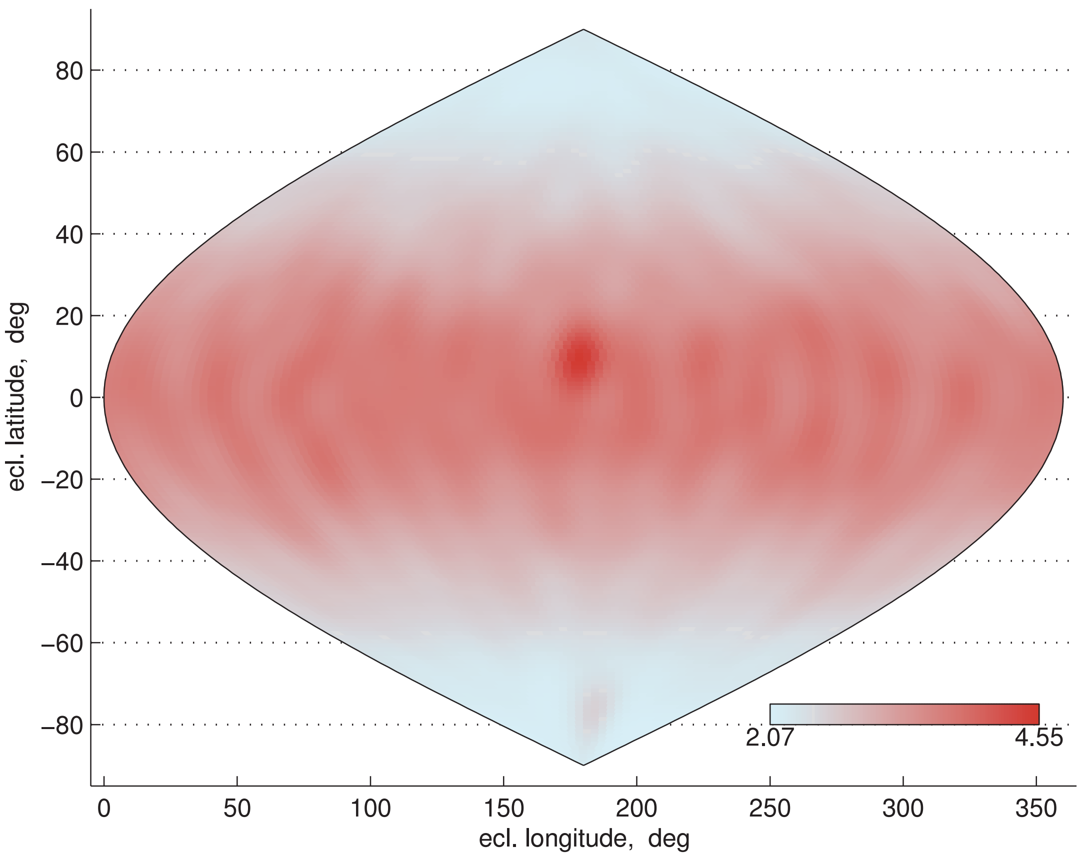

FIG. 4.—Sky distribution of simulated parallax errors (standard deviations) in first 122 spherical harmonics.

ecliptic zone. The pattern of parallax errors of science targets will closely follow that of the grid stars.

10. UNCERTAINTY OF THE MISSION ACCURACY

Each of the 315,000 measurements on grid stars with *SIM* will have a random error due to photon shot noise, metrology errors, etc. The resulting set of astrometric parameters p will also be a random vector. The statistical properties of the astrometric error $e = p_{\rm obs} - p_{\rm true}$ are given by the covariance matrix $C_p = E(e\,e^T)$, which is computed in the global solution. Yet any particular realization of the error e will deviate from the mathematical expectancy. In effect, the overall mission accuracy may be somewhat better or somewhat worse than the statistical mean defined by the covariance matrix. Given (hypothetically) a large number of similar missions, one could verify that the distribution of e has a sample variance very close to the diagonal of C_p. For the only mission that will be implemented, we need to know by what amount the calculated mission accuracy may deviate from the actual performance. In other terms, the question is, what is the sample variance of the variance of astrometric parameters around the diagonal of the covariance matrix?

For simplicity, suppose $\boldsymbol{e}$ is a unit-weight error vector that is drawn from $N(0, 1)$. This does not violate the generality of the following study, since the actual errors can always be normalized by the formal standard deviations. The mission-average astrometric accuracy is defined via the trace of the covariance matrix,

$$\sigma_e = [\mathrm{tr}(C_p)/N]^{1/2}. \tag{63}$$

The actual performance in a single realization is defined by $\sum e_i^2$, which has the expected value $\mathrm{tr}(C_p)$. In Appendix B it is shown that if e_i is normal (as would be the case if the measurement error is normally distributed), then the variance of the former is

$$\begin{aligned} V_e &= E\left\{\left[\sum \boldsymbol{e}_i^2 - \mathrm{tr}(C_p)\right]^2\right\} \\ &= 3\sum v_i^2 - \sum c_{ii}^2 \\ &= 2\sum_i c_{ii}^2 + 3\sum_{i\neq j} c_{ij}^2, \end{aligned} \tag{64}$$

This content downloaded from 150.135.211.221 on Fri, 18 Nov 2016 23:40:02 UTC
All use subject to http://about.jstor.org/terms

where v_i represents the singular values of C_p, and c_{ij} indicates its components.

It is easily verified that the variance V_e depends on the condition number of the covariance matrix $\max(v)/\min(v)$, which is the square of the condition number of the design matrix. Indeed, since $\sum v_i = \sum c_{ii}$, and $\sum v_i^2 = \mathrm{tr}(C_p^T C_p) \geq \sum c_{ii}^2$, the smallest variance V_e is achieved when all v_i are equal, and the condition number is unity (a perfectly conditioned system of equations). Any spread of the singular values and the concomitant increase in condition number of the covariance matrix increases the uncertainty of the actual astrometric performance. Also, as a matter of computation, it is seen that V_e is directly computable from the covariance matrix. From this relationship, it is observed that correlations between parameters also increase the variance of the sampled variance (Appendix B).

The V_e quantity is essentially the variance of the variance. It is more practical to estimate the standard deviation that can be compared with the mission-accuracy estimates. Since the sample variance is a positive statistic with an asymmetric probability distribution function, we found it convenient to use some computable parameters analogous to the relative standard deviation of a normally distributed variable:

$$\sigma_{\mathrm{rms}} = \frac{1}{2} V_e^{1/2}/\mathrm{tr}(C_p). \tag{65}$$

Numerical simulations (including direct computation of the singular values of the full astrometric covariance matrix) produced a σ_{rms} of 11% at the frequency of baseline length update 1/480, which yields a robust, high-accuracy solution. That is to say, if the mission-average positional accuracy is 4 μas, the actual overall rms error is uncertain at 4 ± 0.4 μas.

11. DISCUSSION

We have shown that the current design of the *SIM* can achieve the goal accuracy of 4 μas in positions, parallaxes, and proper motions of grid stars, as far as random uncorrelated errors in delay measurements are concerned. Our simulations include nonastrometric parameters, such as the baseline length and a number of instrument field-dependent calibration parameters. The baseline length is a special parameter, in that the mission performance is sensitive to how often this calibration term has to be solved for. Therefore, the current engineering requirements on the baseline length metrology are set up to meet the astrometric performance goal. The moderate condition of the global grid adjustment with *SIM* due to the lack of a wide calibrating angle is sufficiently well made up for by the extended 15° field of regard of the science interferometer.

Reduction of the grid equations by *QR* factorization of the constant and baseline orientation terms and their subsequent elimination makes it possible to compute the full covariance matrix of the remaining parameters. Coupled with the spherical harmonics analysis, it enables us to investigate in detail the propagation of random errors and the distributions of errors and covariances across the sky. Correlations of astrometric parameters across the sky must be properly accounted for in any astrophysical investigation that uses combinations of astrometric data for a set of stars. This will preclude errors such as those in the computation of the mean parallaxes of open clusters on *Hipparcos* data. Even though the covariance matrix is deterministic, a given mission is a realization and thus may differ from the expectation. We found a way to calculate this basic uncertainty and revealed its relation to the spectrum of singular values of the covariance matrix and the condition of the problem.

The research described in this paper was carried out at the Jet Propulsion Laboratory, California Institute of Technology, under a contract with the National Aeronautics and Space Administration.

APPENDIX A

REDUCTION OF GRID EQUATIONS

In this appendix, a more transparent motivation and justification for the grid reduction is presented.

Retaining the previous notations, we begin with equation (12), suppressing the dependence on the baseline length and the tile number:

$$\boldsymbol{\delta}_j = \langle \boldsymbol{b}^0 \times \boldsymbol{s}_j^0, \boldsymbol{\omega} \rangle - \langle \boldsymbol{b}^0 \times \boldsymbol{s}_j^0, \boldsymbol{\omega}_j \rangle + c; \quad j = 1, \ldots, N, \tag{A1}$$

where N is the number of stars in the tile. The basic idea is to eliminate the unknowns $\boldsymbol{\omega}$ and c directly from this set of equations. To this end, we define for each j,

$$\boldsymbol{v}_j = \boldsymbol{b}^0 \times \boldsymbol{s}_j^0 \tag{A2}$$

and observe that in general, $\{\boldsymbol{v}_j\}_{j=1}^N$ spans the two-dimensional subspace orthogonal to $\boldsymbol{b}^0$, and each vector $\boldsymbol{v}_j$ is in this subspace. Thus, in general, the set of vectors $\{\boldsymbol{V}_j\}_{j=1}^N$,

$$\boldsymbol{V}_j = \begin{bmatrix} \boldsymbol{v}_j \\ 1 \end{bmatrix}, \tag{A3}$$

spans a three-dimensional subspace. Without loss of generality,

This content downloaded from 150.135.211.221 on Fri, 18 Nov 2016 23:40:02 UTC
All use subject to http://about.jstor.org/terms

we assume the equations have been ordered so that $\boldsymbol{V}_1$, $\boldsymbol{V}_2$, and $\boldsymbol{V}_3$ are independent.[4] Then for any $j > 3$, there exist unique scalars α_j, β_j, and $\boldsymbol{\gamma}_j$ such that

$$\boldsymbol{V}_j = \alpha_j \boldsymbol{V}_1 + \beta_j \boldsymbol{V}_2 + \boldsymbol{\gamma}_j \boldsymbol{V}_3. \tag{A4}$$

Defining for each $j > 3$,

$$\tilde{\boldsymbol{\delta}}_j = \boldsymbol{\delta}_j - [\alpha_j \boldsymbol{\delta}_1 + \beta_j \boldsymbol{\delta}_2 + \boldsymbol{\gamma}_j \boldsymbol{\delta}_3], \tag{A5}$$

the system of equations

$$\tilde{\boldsymbol{\delta}}_j = -\langle \boldsymbol{v}_j, \boldsymbol{\omega}_j \rangle + [\alpha_j \langle \boldsymbol{v}_1, \boldsymbol{\omega}_1 \rangle + \beta_j \langle \boldsymbol{v}_2, \boldsymbol{\omega}_2 \rangle + \boldsymbol{\gamma}_j \langle \boldsymbol{v}_3, \boldsymbol{\omega}_3 \rangle],$$
$$j = 4, \ \ldots, N \tag{A6}$$

results from equation (A1), with the $\boldsymbol{\omega}$ and c terms having been removed. This process can be performed on each tile, thereby globally eliminating all the baseline rotation vectors and constant terms.

The particular motivation for using the QR factorization in the algorithm principally stems from the following observation. In matrix notation, we recast equation (A1) as

$$\boldsymbol{\delta} = A \begin{bmatrix} \boldsymbol{x} \\ \boldsymbol{y} \end{bmatrix}, \tag{A7}$$

where $\boldsymbol{\delta}$ is the vector of measurements, $\boldsymbol{x}$ is the vector of "instrument" parameters ($\boldsymbol{\omega}$ and c), and $\boldsymbol{y}$ is the vector of star direction update parameters. Using the elementary row operations defined by equation (A5) leads to

$$E\boldsymbol{\delta} = EA \begin{bmatrix} \boldsymbol{x} \\ \boldsymbol{y} \end{bmatrix}, \tag{A8}$$

where E is the matrix of these operations. Now $E\boldsymbol{\delta}$ can be partitioned as

$$E\boldsymbol{\delta} = \begin{bmatrix} \boldsymbol{\delta}_1 \\ \boldsymbol{\delta}_2 \\ \boldsymbol{\delta}_3 \\ \tilde{\boldsymbol{\delta}} \end{bmatrix}, \tag{A9}$$

and correspondingly, EA is partitioned as

$$EA = \begin{bmatrix} A_1 & A_2 \\ 0 & A_3 \end{bmatrix}. \tag{A10}$$

The astrometric parameters appear without the instrument parameters in the lower part of the partitioned equation defined by equations (A8) and (A9). The specific system of interest is

$$\tilde{\boldsymbol{\delta}} = A_3 \boldsymbol{y} \tag{A11}$$

in this context.

A more proper formulation of the delay equation (A1) would include a noise vector term. The standard assumption is that the noise on the observations are uncorrelated, mostly resulting from photon statistics and other uncorrelated time-varying phenomena, while systematic errors must be treated differently. Performing the row-operation matrix E changes the covariance of the noise vector. Using the QR factorization avoids having to account for the covariance matrices on each tile.

[4] In the pathological case that the $\{\boldsymbol{V}_j\}$ only span a two-dimensional subspace, then we only need to take $\boldsymbol{V}_1$ and $\boldsymbol{V}_2$ as the spanning set.

APPENDIX B

VARIANCE OF MISSION ACCURACY CALCULATION

Let P denote an $N \times N$ error covariance matrix. This may include all of the instrument parameters or just a subset of them (e.g., parallax). We assume here that the P is generated from measurement errors that have a Gaussian distribution. Hence, P is uniquely associated with a zero mean random N-vector that is normally distributed with covariance matrix P. Let x denote an N-vector sample from this distribution, and let

$$\boldsymbol{z} = \sum_{i=1}^{N} \boldsymbol{x}_i^2. \tag{B1}$$

Then z is an unbiased estimate of $\mathrm{tr}(P)$, since

$$\begin{aligned} E(\boldsymbol{z}) &= \sum E(\boldsymbol{x}_i^2) \\ &= \sum \sigma_i^2 \\ &= \mathrm{tr}(P). \end{aligned} \tag{B2}$$

Since P is symmetric, can be diagonalized by an orthogonal matrix U such that $D = UPU^T$ is diagonal, with entries d_i on the diagonal. Now we introduce the random variables $\boldsymbol{y}_i$,

This content downloaded from 150.135.211.221 on Fri, 18 Nov 2016 23:40:02 UTC
All use subject to http://about.jstor.org/terms

$i = 1, \ldots, N$:

$$y_i = \sum_{j=1}^{N} U_{ij} x_j \tag{B3}$$

and observe that

$$\begin{aligned} E(y_i y_k) &= E(\sum_j U_{ij} x_j \sum_l U_{kl} x_l) \\ &= \sum U_{ij} P_{jl} U_{kl}, \quad \text{since} \quad E(x_j x_l) = P_{jl} \\ &= \delta_{ik} d_k. \end{aligned} \tag{B4}$$

Note that y_i now represents independent zero-mean Gaussian random variables with variance d_i. Also observe that since U is orthogonal, $|y|^2 = |Ux|^2 = |x|^2$; i.e.,

$$\sum_i y_i^2 = \sum_i x_i^2. \tag{B5}$$

With these observations, we can now compute the variance of the estimate z:

$$\begin{aligned} E\{[z - \mathrm{tr}(P)]^2\} &= E[z^2 - 2z\mathrm{tr}(P) + \mathrm{tr}(P)^2] \\ &= E[z^2 - \mathrm{tr}(P)^2]. \end{aligned} \tag{B6}$$

However,

$$\begin{aligned} E(z^2) &= E[(\sum_i y_i^2)^2] \\ &= \sum_{i \neq j} E(y_i^2)E(y_j^2) + \sum_i E(y_i^4) \\ &\quad \text{using independence} \\ &= \mathrm{tr}(P)^2 - \sum_i P_{ii}^2 + \sum_i E(y_i^4). \end{aligned} \tag{B7}$$

Hence,

$$E\{[z - \mathrm{tr}(P)]^2\} = \sum_i E(y_i^4) - \sum_i P_{ii}^2. \tag{B8}$$

But since y_i is Gaussian, $E(y_i^4) = 3d_i^2$. Therefore,

$$E\{[z - \mathrm{tr}(P)]^2\} = \sum_i 3d_i^2 - \sum_i P_{ii}^2. \tag{B9}$$

Next observe that by applying the spectral theorem, the eigenvalues of P^2 are d_i^2. Hence,

$$E\{[z - \mathrm{tr}(P)]^2\} = 3\mathrm{tr}(P^2) - \sum_i P_{ii}^2. \tag{B10}$$

This relationship clarifies the role that correlations have in increasing the sampled variance. Specifically, since

$$\mathrm{tr}(P^2) = \sum_{ij} P_{ij}^2, \tag{B11}$$

it follows that

$$E\{[z - \mathrm{tr}(P)]^2\} = 2\sum_i P_{ii}^2 + 3\sum_{i \neq j} P_{ij}^2. \tag{B12}$$

REFERENCES

Arenou, F., et al. 1995, A&A, 304, 52
Arfken, G. B., & Weber, H. J. 1995, Mathematical Methods for Physicists (4th ed.; New York: Academic Press)
Boden, A. F. 1997, JPL Internal Rep. D-32267 (Pasadena: JPL)
Bucciarelli, B., et al. 1991, Adv. Space Res., 11, 79
de Vegt, Chr., & Ebner, H. 1974, MNRAS, 167, 169
Eichhorn, H. 1960, Astron. Nachr., 285, 233
ESA. 1997, The *Hipparcos* Catalogue (ESA SP-1200; Noordwijk: ESA)
Golub, G., & Van Loan, C. F. 1989, Matrix Computations (Baltimore: Johns Hopkins Univ. Press)
Googe, W. D., Eichhorn, H., & Lukac, C. F. 1970, MNRAS, 150, 35
Halmos, P. R. 1982, A Hilbert Space Problem Book (2nd ed.; New York: Springer)
Hanson, R. B. 1980, MNRAS, 192, 347
Jefferys, W. H. 1963, AJ, 68, 111
Laskin, R. A. 2003, Proc. SPIE, 4852, 16
Lattanzi, M. G., Bucciarelli, B., & Bernacca, P. L. 1990, ApJS, 73, 481
Loiseau, S., & Malbet, F. 1996, A&AS, 116, 373
Makarov, V. V. 1998, A&A, 340, 309
———. 2002, AJ, 124, 3299
———. 2003, AJ, 126, 2408
Milman, M. H. 2003, JPL Internal Rep. D-32266 (Pasadena: JPL)
Milman, M. H., & Turyshev, S. G. 2000, Proc. SPIE, 4006, 828
Murphy, D. W., & Meier, D. L. 2004, Proc. SPIE, 5497, 577
Pinsonneault, M. H., Stauffer, J., Soderblom, D., King, J. R., & Hanson, R. B. 1998, ApJ, 504, 170
Shao, M. 1998, Proc. SPIE, 3350, 536
Swartz, R. 2003, Proc. SPIE, 4852, 100
Unwin, S. C., & Shao, M. 2000, Proc. SPIE, 4006, 754

This content downloaded from 150.135.211.221 on Fri, 18 Nov 2016 23:40:02 UTC
All use subject to http://about.jstor.org/terms